substance: boron compounds
property: structural properties of hexaborides with B_6 octahedra

The unit cell of the cubic structure contains one formula weight of MB_6 (Fig. 1). The boron atoms form regular octahedra positioned at the corners of the unit cell, whose center is occupied by the metal atom. All rare-earth metals and moreover Ca, Sr, Ba, Tl and Pu form isostructural hexaborides (see [77E)]. Often these structures are denoted as CaB_6-type.

Alkali hexaborides are semiconductors. Hexaborides with divalent metals have been predicted to be semiconductors or insulators, while hexaborides with trivalent metals are assumed to be metallic. Sm ions exhibit an intermediate valence.

Representatives of metal hexaborides [94K, 85E]

(d_{M-M}, metal-metal interatomic distance; r_M, metallic radii sum; d_{M-M}, r_M in Å)

Compound	d_{M-M}	$\Delta = a - 2r_M$	Conductivity type	
$M^{+1}B_6$				
NaB_6				54B
$Na_xBa_{1-x}B_6$				76N
$Na_xTh_{1-x}B_6$				76N
NaB_5C				98A
$M^{+2}B_6$				
CaB_6	4.1525	0.204	semiconductor	86I
SrB_6	4.1897	–0.114	semiconductor	92C
BaB_6	4.269	–0.077	semiconductor	77N
EuB_6	4.1849	0.195	semiconductor	95B
YbB_6	4.1479	0.268	semiconductor	95B
LaB_6				82B
TbB_6				82B
GdB_6				83S
NdB_6				83S
PrB_6				79P
$Sm^{+2.6}B_6$ (intermediate valence)				
SmB_6	4.1332	0.513	gap at E_F	93T
$M^{+3}B_6$				
YB_6	4.113	0.493	metal	77N
LaB_6	4.1466	0.419	metal	93O
CeB_6	4.1396	0.500	metal	89B
PrB_6	4.1319	0.492	metal	92C
NdB_6	4.1259	0.498	metal	94M, 95B
$M^{+4}B_6$				
ThB_6	4.1105	0.510	metal	77N

Lattice parameters of metal hexaborides compared with the atomic radii of the metal atoms in Fig. 2 [87P].

Lattice parameters of metal hexaborides (lattice constants, bond lengths, mean square displacement) in Figs. 3 and 4 [99T].

X-ray diffraction of CaB_6, LaB_6, YbB_6 and ThB_6 in [82B].

MeB_6 lattice constant depending on the metal atomic number in [87P].

Preparation with the aluminium-flux method [83G].

Temperature dependence of the lattice parameters of CaB_6, $Sm_{0.05}Ca_{0.95}B_6$, $Sm_{0.4}Ca_{0.6}B_6$, SmB_6,

$Sm_{0.5}La_{0.5}B_6$, LaB_6 determined by neutron scattering in Fig. 5 [88A, 91A].

Comparison of calculated and measured lattice constants and interoctahedral B-B distances in [97R].

Correlation between B charge and valence electron concentration in Fig. 6 [97R].

Lattice distortion in mixed crystals of some rare earth hexaborides [99K1].

Preparation of hexaborides solid solution single crystals by zone melting [99K2].

Force constants for some hexaborides [mdyn $Å^{-1}$] [90Y]. (numerical parameters of a MVFF treatment to fit the observed IR and Raman spectra).

Compound	B – B intraocta-hedral	Bond-bond 60°	Bond-bond 90°	Bond-bond non ‖	Bond-bond ‖	M – B	B – B interocta-hedral	B – B – B bend 135°
CaB_6	1.464	0.147	–0.071	–0.184	–0.325	0.192	1.708	0.275
SrB_6	1.278	0.148	–0.022	–0.135	–0.269	0.180	1.395	0.589
LaB_6	1.348	0.145	–0.033	–0.174	–0.337	0.144	1.664	0.168
NdB_6	1.434	0.150	–0.038	–0.175	–0.334	0.113	1, 743	0.174
GdB_6	1.503	0.156	–0.058	–0.179	–0.428	0.095	1.827	0.190
TbB_6	1.560	0.159	–0.060	–0.179	–0.490	0.096	1.860	0.195
DyB_6	1.614	0.175	–0.087	–0.180	–0.510	0.089	1.885	0.220
YbB_6	1.408	0.147	–0.062	–0.174	–0.302	0.185	1.688	0.428

The magnitude of the ^{11}B nuclear electric quadrupole interaction in divalent and trivalent-metal hexaborides and mixed-valent SmB_6 depending on the lattice parameter in Fig. 7 [86B].

Linear relation between the variation in the interoctahedral B-B force constant and the lattice constant in [93N].

Work function and effective magnetic moment in Fig. 8 [59S].

Reflectivity spectra of LaB_6, SmB_6, EuB_6 up to 42 eV in Fig. 9 [81S].

Reflectivity spectra of pure YB_6, LaB_6, CeB_6, SmB_6, $Sm_{0.8}B_6$ and TbB_6 in Fig. 10 [99W].

Spectroscopic investigation of lattice vacancies in hexaborides [93B].

IR diffuse reflectance spectra of MB_6 compounds with two-valent Yb, Sr and Ca and three-valent Nd, Gd, La, and Dy metal atoms in Fig. 11 [88T, 93Y].

Representative Raman spectra of hexaborides with twofold and threefold ionized metal atoms in Fig. 12 [88T, 93Y].

Frequencies of the phonon symmetry modes A_{1g}, E_g, T_{2g} and T_{1u} for several metal hexaborides in Fig. 13 [86Z].

Phonon frequencies from IR absorption vs. lattice parameter of some metal hexaborides in Fig. 14 [99W].

Magnetic susceptibility of DyB_6, TbB_6 and HoB_6 in Fig. 15 [97T].

Thermal conductivity and magnetic susceptibility of alkali and rare earth hexaborides in [65L].

Observed vibrational wavenumbers ν/c (in cm^{-1}) of metal hexaborides [93Y].

SrB_6		**YbB_6**		**CaB_6**		**DyB_6**		
Raman	IR	Raman	IR	Raman	IR	Raman	IR	Assignments
1400	1450	1400	1480	1475	1430	1510	1470	ν_5+tr (comb)
1300	1330	1340	1310	1500	1340	1400	1330	
1225	1200	1258 s	1200	1270 s	1260	1314 s	1310	ν_1 A_{1g} (s)
	1190		1170... 1090		1125... 1095		1160... 1100	ν_2 F_{1u} (b)
	1085							
	1020							
1192 sh		1160 sh		1154 sh		1160 w		ν_2 E_g (s)

1105		1122 m		1125 s		1180 s		
1078								
		1091 m						
		1081 w						
			960... 810	960	800 m	935 w		ν_7 F_{2u} (b)
				845 w		860 w	792	
	730... 685		740... 685					
770 s		760 s		775 s		773 m		ν_4 F_{2g} (b)
752 sh		732 sh		762 sh		715 sh		
730								
685								
470 w	480	510 w	520	526 w	520	500 w	480	ν_3 F_{1g} (r)
465 w	475	420 w	460	485 w	470		475	
128		250		330		262		ν_6 F_{1u} (t)
		150		250		180		

TbB_6		**GdB_6**		**NdB_6**		**LaB_6**		
Raman	IR	Raman	IR	Raman	IR	Raman	IR	Assignments
1460	1410	1430	1430	1490	1480	1440	1430	ν_5+tr (comb)
1380	1375	1350	1330	1395	1320	1330	1340	
1298	1280	1290 s	1260	1285 s	1260	1242	1240	ν_1 A_{1g} (s)
	1155... 1085		1160... 1100		1165... 1095		1170... 1095	ν_2 F_{1u} (b)
1168 s		1156 w		1145 s		1152 s		ν_2 E_g (s)
1100 sh	1142 w		1136 sh		1112 sh			
918 w	806	940 w		928	790		790	ν_7 F_{2u} (b)
845 w	790	842 w	790	778	690		700	
			680					
715 sh		680 w		685 s		782 w		ν_4 F_{2g} (b)
692 m						690 sh		
						670 m		
	490		523	560 w	500	500 w	533	ν_3 F_{1g} (r)
		480	460	530	460			
248		242				210		ν_6 F_{1u} (t)
185				175		170		

s = strong; m = medium; w = weak; sh = shoulder; (s) = stretch; (b) = bend; (r) = rotation; (t) = translation

Multichannel Raman studies of binary alkaline borides MB_6 (M = Ca, La, Sr, Sm) (abstract only) in [86Y].

The micromechanical properties of metal hexaborides [79P].

Study of the electronic structure of rare earth hexaborides (La, Ce, Pr, Nd, Sm, Eu, Gd, Yb, Y) [85G].

Phonon and specific heat analysis in rare-earth hexaborides [99K2].

Charge carriers per Ln atom derived from Hall effect and XCS (X-ray chemical shift) measurements

Compound	*n*(Hall)	*n*(XCS)

LaB_6	0.93	0.86(3)	85G
CeB_6	1.06	1.00(5)	
NdB_6	0.88	1.01(5)	
PrB_6	0.84	0.82(8)	
EuB_6	0.03	≤ 0.05	
GdB_6	0.94	1.0(1)	
YbB_6	0.05	≤ 0.05	
YB_6	0.96	1.00(2)	

Bipolaron formation in icosahedral and octahedral borides [98E].

Pressure dependence of the electrical resistivity; $\rho(p)/\rho(0)$ vs. hydrostatic pressure p for some metal hexaborides in Fig. 16 [81K, 91S].

Pressure dependence of the thermoelectric power S for LaB_6, YbB_6 and EuB_6 in Fig. 17 [81K].

Vacancies and thermal vibrations of atoms in the crystal structure of rare earth hexaborides [94K].

Boron-boron bond lengths vs. lattice parameter for some metal hexaborides in Fig. 18 [94K].

Characteristic Einstein temperatures of the RE atoms vs. atomic number of the RE element in Fig. 19 [94K].

Variation of the atomic equivalent temperature factors (normalized by a^2) vs. the atomic number of the RE element in Fig. 20 [94K, 99T.

Entropy of LaB_6, ferromagnetic EuB_6 and antiferromagnetic EuB_6 in Fig. 21 [80F].

The working reliability and structure stability of thermoemission lanthanum hexaboride elements in stationary plasma thruster hollow cathode [98P].

High temperature hardness of single crystals of LaB_6, CeB_6, PrB_6, NdB_6 and SmB_6 [99O].

Review papers

General review article [85E].

On the physical properties of intermediate valent hexa- and dodecaborides [87W].

On band structure calculations of metal hexaborides [87A].

References:

54B Blum, P., Bertraut, F.: Acta Crystallogr. 7 (1954) 81.

59S Samsonov, G.V., Shravlev, N.N., Paderno, Yu.B., Melik-Adamyai, V.R.: Kristallografiya 4 (1959) 538 (in Russian).

65L L'vov, C.H., Nemtchenko, V.F., Paderno, Yu.B.: in: Vsokotemperaturnaye neorganicheskie soednienia, Nauka Dumka ed., Kiev, 1965, p. 445 (in Russian).

76N Naslain, P., Guette, A,, Hagenmuller, P.: J. Less-Common Met. 47 (1976) 1.

77E Etourneau, J., Mercurio, J.P., Hagenmuller, P.: in: Boron and Refractory Borides, V.I Matkovich ed., Springer: Berlin, Heidelberg, New York, 1977, p. 115.

77N Naslain, R., Etourneau, J., Hagenmuller, P.: in: Boron and Refractory Borides, V.I. Matkovich ed., Springer: Berlin, Heidelberg, New York, 1977, p. 262.

79A Aono, M., Kawai, S.: J. Phys. Chem. Solids 40 (1979) 797.

79P Paderno, V.N., Paderno, Yu.B., Pilyankevich, A.N., Lazorenko, V.I., Bulychev, S.I.: J. Less-Common Met. 67 (1979) 431.

80F Fujita, T., Suzuki, M., Isikawa, Y.: Solid State Commun. 33 (1980) 947.

81K Korsukova, M.M., Stepanov, N.N., Gontcharova, E.V., Gurin, V.N., Nikanorov, S.P., Smirnov, I.A.: J. Less-Common Met. 82 (1981) 211. (Proc. 7th Int. Symp. Boron, Borides and Rel. Compounds, Uppsala, Sweden, 1981).

81S Shelykh, A.I., Sidorin, K.K., Karin, M.G., Bobrikov, V.N., Korsukova, M.M., Gurin, V.N., Smirnov, I.A.: J. Less-Common Met. 82 (1981) 291.

82B Barantseva, I.G., Paderno, Yu.B.: Sov. Powder Metall. Met. Ceram. 21 (1982) 585.

83G Gurin, V.N., Korsukova, M.M.: Prog. Cryst. Growth and Charact. 6 (1983) 59.

83S Storms, E.K.: J. Appl. Phys. 54 (1983) 1076.

85E Etourneau, J., Hagenmuller, P.: Philos. Mag. 52 (1985) 589.

85G Grushko, Yu.S., Paderno, Yu.B., Mishin, K.Ya., Molkanov, L.I., Shadrina, G.A., Konovalova, E.S., Dudnik, E.M.: Phys. Status Solidi (b) 128 (1985) 591.

86B Bray, P.J.: in: Boron-Rich Solids (AIP Conf. Proc. 140), Albuquerque, New Mexico 1985, D. Emin, T.L. Aselage, C.L. Beckel, I.A. Howard ed., American Institute of Physics: New York, 1986, p. 142.

86I Ito, T., Higashi, I.: Chem. Sci. 26 (1986) 479.

86Y Yahia, Z., Turrell, S., Dhamlincourt, M.-C., Turrell, G.: in: Proc. 10th Int. Conf. Raman spectroscopy 86, Eugene, OR, USA,, Peticolas, W.L.; Hudson, B.; ed., Univ. Oregon: Eugene, OR, USA, 1986, p. 11(abstract only).

86Z Zirngiebl, E., Blumenröder, S., Mock, R., Güntherodt, G.: J. Magn. Magn. Mater. 54-57 (1986) 359.

87A Armstrong, D.R.: in: Proc. 9th Int. Symp. Boron, Borides and Rel. Compounds, University of Duisburg, Germany, Sept. 21 - 25, 1987, H. Werheit ed., University of Duisburg: Duisburg, 1987, p. 125.

87P Paderno, Yu.B., Konovalova, E.S.: in: Proc. 9th Int. Symp. Boron, Borides and Rel. Compounds, University of Duisburg, Germany, Sept. 21 - 25, 1987, H. Werheit ed., University of Duisburg: Duisburg, 1987, p. 65.

87W Wachter, P.: in: Proc. 9th Int. Symp. Boron, Borides and Rel. Compounds, University of Duisburg, Germany, Sept. 21 - 25, 1987, H. Werheit ed., University of Duisburg: Duisburg, 1987, p. 166.

88A Alekseev, P.A., Konovalova, E.S., Lasukov, V.N., Lyukshina, S.I., Paderno, Yu.B., Sadikov, I.P., Udovenko, E.V.: Fiz. Tverd. Tela 30 (1988) 2024 (in Russian).

88T Turrell, S., Yahia, Z., Huvenne, J.P., Lacroix, B., Turrell, G.: J. Mol. Struct. 174 (1988) 455.

89B Blomberg, M.K., Merisalo, M.J., Korsukova, M.M., Gurin, V.N.: J. Less-Common Met. 146 (1989) 309.

90Y Yahia, Z., Turrell, S., Turrell, G., Mercurio, J.P.: J. Mol. Struct. 224 (1990) 303.

91A Alekseev, P.A., Ivanov, A.S., Kikoin, K.A., Mischenko, A.S., Lazukov, A.N., Rumyantsev, A.Yu., Sadikov, I.P., Konovalova, E.S., Paderno, Yu.B.: in: Boron-Rich Solids, Proc. 10th Int. Symp. Boron, Borides and Rel. Compounds, Albuquerque, NM 1990 (AIP Conf. Proc. 231), D. Emin, T.L. Aselage, A.C. Switendick, B. Morosin, C.L. Beckel ed., American Institute of Physics: New York, 1991, p. 318.

91S Sidorov, V.A., Stepanov, N.N., Ziok, O.B., Chvostanzev, L.G., Smirnov, N.A., Korsukova, M.M.: Fiz. Tverd. Tela 33 (1991) 1271(in Russian).

92C Chernychev, V.V., Aslanov, L.A., Korsukova, M.M., Gurin, V.N.: (cited in 94K 11).

93B Bat'ko, I., Flachbart, K., Mat'as, S., Paderno, Yu.B., Shicevalova, N.Yu.: J. Alloys Compounds 196 (1993) 133.

93N Nagao, T., Kitamura, K., Iizuka, Y., Oshima, C., Otani, S.: Surf. Sci. 290 (1993) 436.

93O Otani, S., Honma, S., Yajima, Y., Ishizawa, Y.: J. Cryst. Growth 126 (1993) 466.

93T Trounov, V.A., Malyshec, A.L., Chernyshov, D.Yu., Korsukonva, M.M., Gurin, V.N., Aslanov, L.A., Chernychev, V.V.: J. Phys.: Condens. Matter 5 (1993) 2479.

93Y Yahia, Z., Turrel, S., Mercurio, J.P., Turrel, G.: J. Raman Spectroscopy 24 (1993) 207.

94K Korsukova, M.M.: Proc. 11th Int. Symp. Boron, Borides and Rel. Compounds, Tsukuba, Japan, August 22 - 26, 1993, Jpn. J. Appl. Phys. Series 10 (1994), p. 15.

94M Malyshev, A., Chernyshov, D., Trounov, V., Gurin, V.N., Korsukova, M.M.: Proc. 11th Int. Symp. Boron, Borides and Rel. Compounds, Tsukuba, Japan, August 22 - 26, 1993, Jpn. J. Appl. Phys. Series 10 (1994), p. 19.

95B Blomberg, M.K., Merisalo, M.J., Korsukova, M.M., Gurin, V.N.: J. Alloys Compounds 217 (1995) 123.

97R Ripplinger, H., Schwarz, K., Blaha, P.: J. Solid State Chem. 133 (1997) 51 (Proc. 12th Int. Symp. Boron, Borides and Rel. Compounds, Baden, Austria, 1996).

97T Takahashi, K., Kunii, S.: J. Solid State Chem. 133 (1997) 198 (Proc. 12th Int. Symp. Boron, Borides and Rel. Compounds, Baden, Austria, 1996).

98A Albert, B., Schmitt, K.: Chem. Commun. (1998) 2373.

98E Emin, D.G., Evans, S.S., McCready, S.S.: Phys. Status Solidi (b) 205 (1998) 311.

98P Paderno, V.N., Paderno, Yu.B., Filippov, V.B., Arkhipov, B.A.: J. Mater. Process. Manufact. Sci. 6 (1998) 311.

99K2 Konovalova, E., Paderno, Yu.B.: J. Solid State Chem. (2000) (Proc. 13th Int. Symp. Boron, Borides and Rel. Compounds, Dinard, France, Sept. 1999).

99K1 Korsukova, M.M., Gurin, V.N., Vegas, A., Gonzalez-Calbert, J.M., Otani, S.: J. Solid State Chem. (2000) (Proc. 13th Int. Symp. Boron, Borides and Rel. Compounds, Dinard, France, Sept. 1999).

99K2 Kunii, S., Takahashi, K., Iwashita, K.: J. Solid State Chem. (2000) (Proc. 13th Int. Symp. Boron, Borides and Rel. Compounds, Dinard, France, Sept. 1999).

99O Oku, T., Bovin, J.-O., Higashi, I., Tanaka, T., Ishizawa, Y.: J. Solid State Chem. (2000) (Proc. 13th Int. Symp. Boron, Borides and Rel. Compounds, Dinard, France, Sept. 1999).

99T Takahashi, Y., Ohshima, K., Okamura, F.P., Otani, S., Tanaka, T.: J. Phys. Soc. Jpn. 68 (1999) 2304.

99W Werheit, H., Au, T., Schmechel, R., Paderno, Yu.B., Konovalova, E.S.: J. Solid State Chem. (2000) (Proc. 13th Int. Symp. Boron, Borides and Rel. Compounds, Dinard, France, Sept. 1999).

Fig. 1.

Metal hexaborides. Unit cell with B_6 octahedra at the corners and the metal (M) atom in the center.

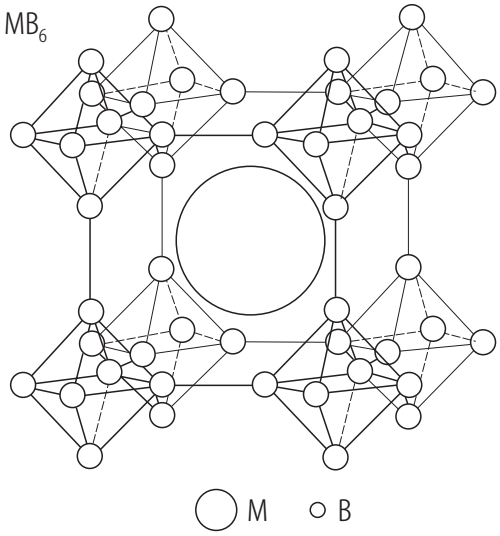

Fig. 2.

Metal hexaborides. Lattice parameters of metal hexaborides (lower curve) vs. atomic number of the metal atoms compared with the atomic radii of the metal atoms (upper curve) [87P].

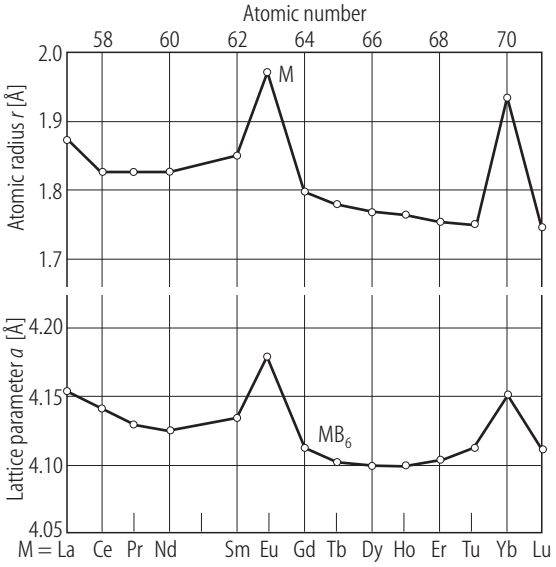

Fig. 3.

Metal hexaborides. Lattice parameters of metal hexaborides vs. atomic number; **(a)** boron coordinate X_B; **(b)** lattice constant; **(c)** bond length between rare earth metal and boron atom; **(d)** intra-octahedral and inter-octrahedral bond lengths; **(e)** quantities of the temperature parameters for the mean square displacement of atoms: circles at 295 K, U_{iso} for the rare earth metal atoms; down triangles, $U_{22=33}$ for the boron atoms; up triangle, U_{11} for the boron atoms [99T].

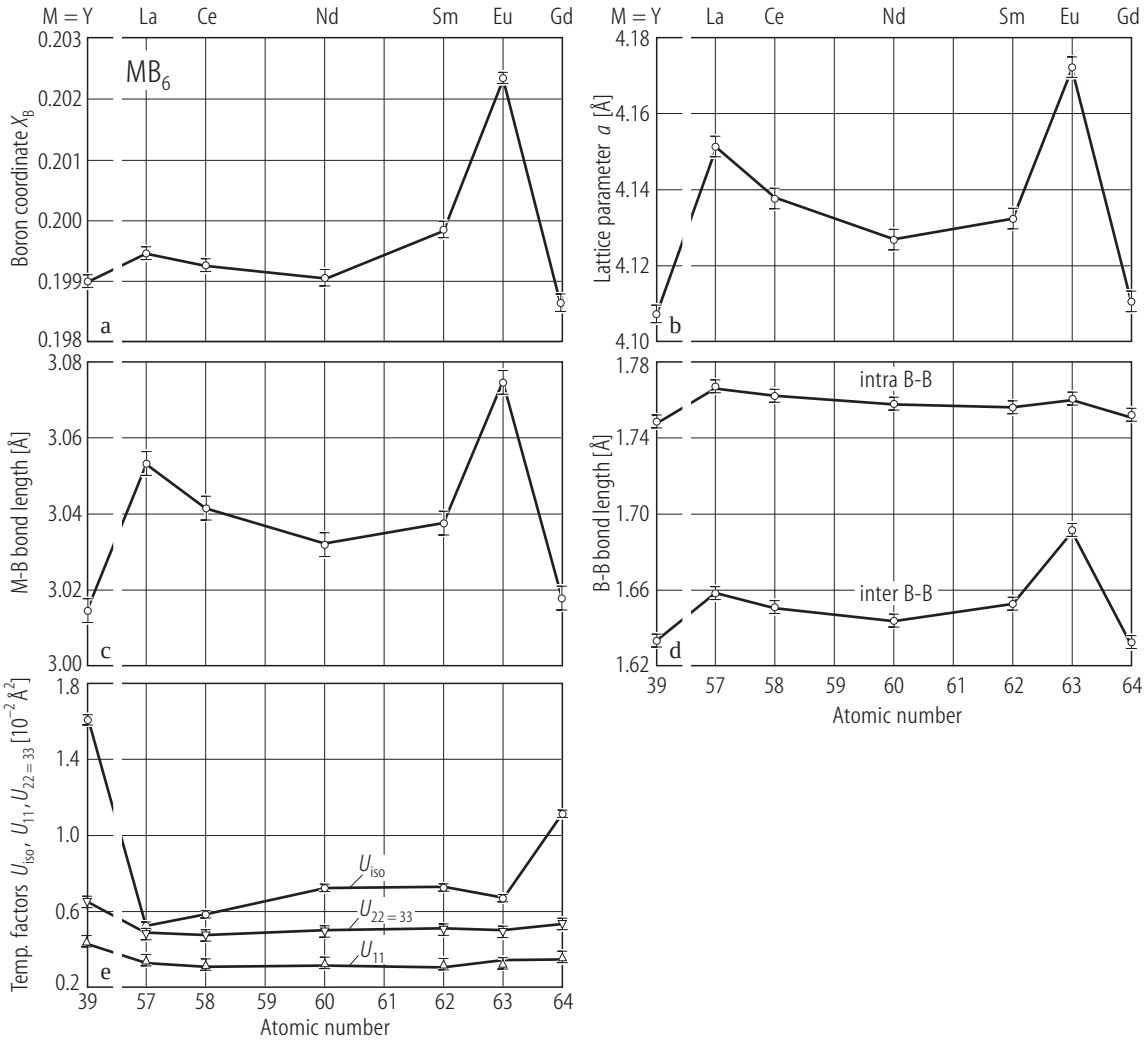

Fig. 4.

Metal hexaborides. **(a)** Ionic radius of the RE ions; **(b)** intra-octahedral and inter-octrahedral bond lengths and **(c)** square root for U_{iso} for the rare earth metal atoms vs. lattice parameter [99T].

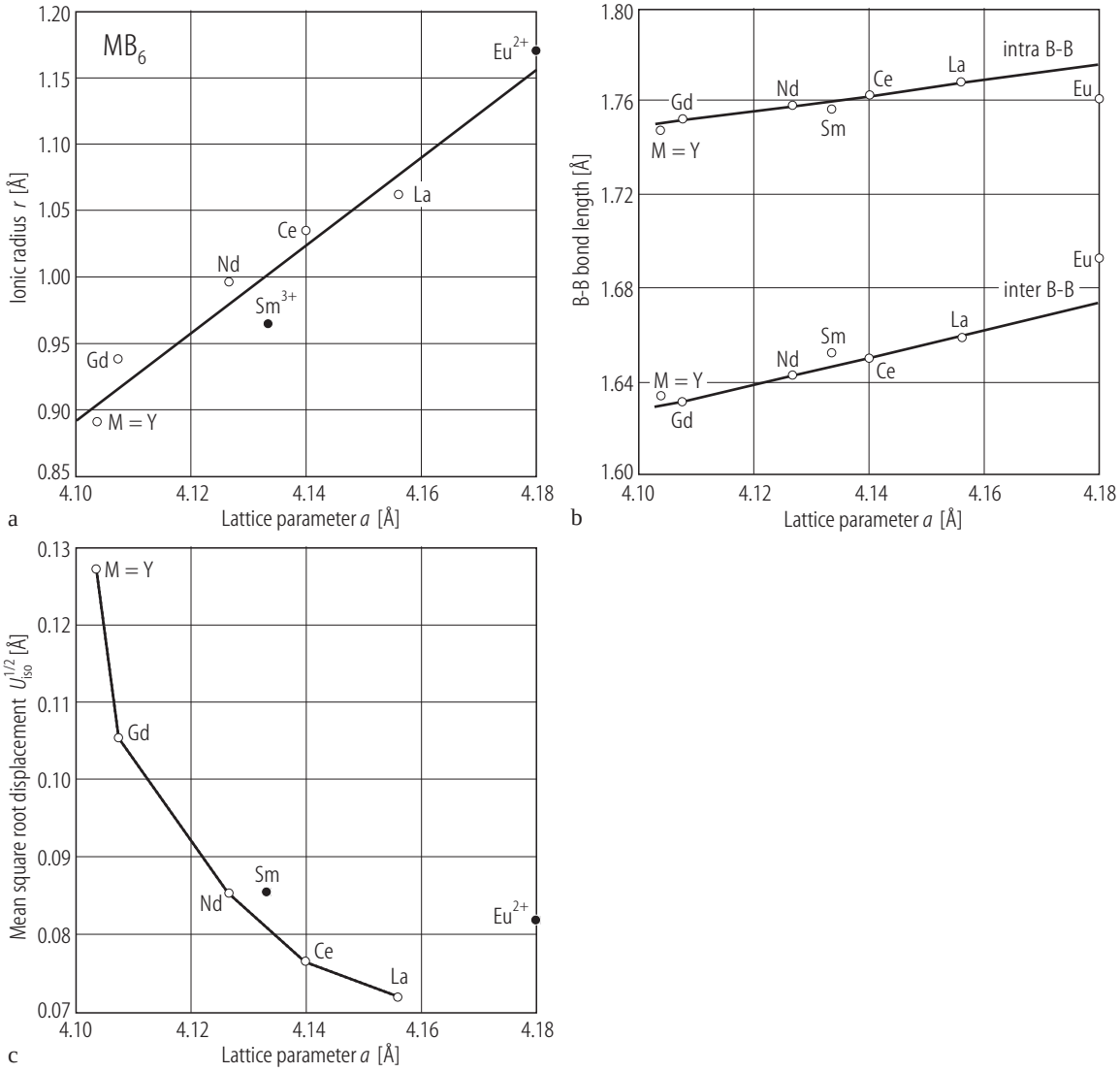

Fig. 5.

Metal hexaborides. Temperature dependence of the lattice parameters of CaB_6, $Sm_{0.05}Ca_{0.95}B_6$, $Sm_{0.4}Ca_{0.6}B_6$, SmB_6, $Sm_{0.5}La_{0.5}B_6$, LaB_6 determined by neutron scattering in [88A, 91A].

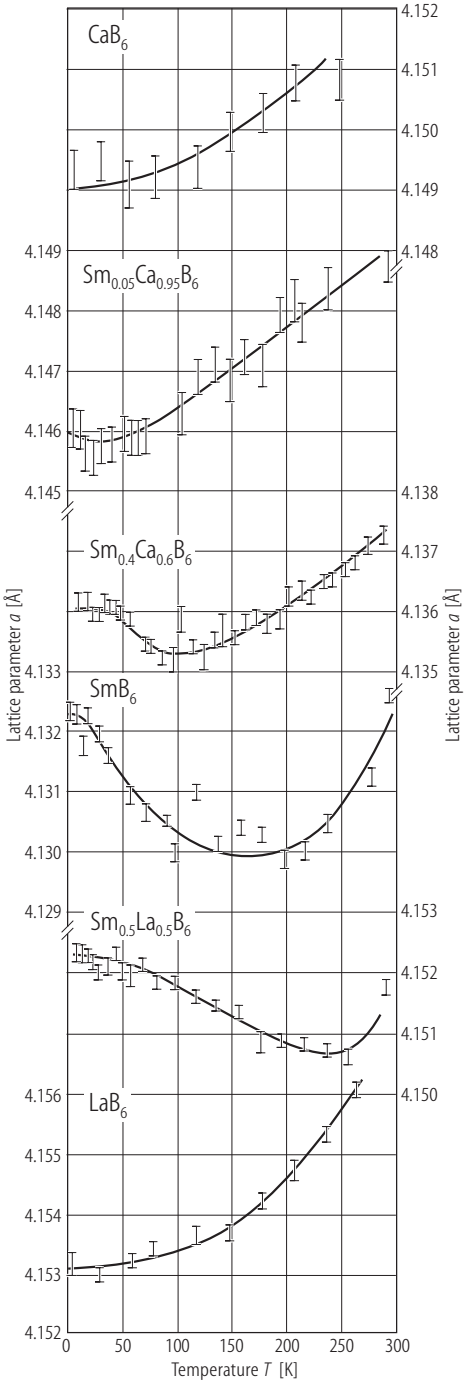

Fig. 6.

Metal hexaborides. Correlation between B charge and VEC, the valence electron concentration (number of valence electrons per unit cell volume). The B charge is determined as the valence charge inside the boron sphere (with r_B = 0.794 Å). Assuming localized 4f states for La and Ce or 4d states for Y makes these atoms divalent [97R].

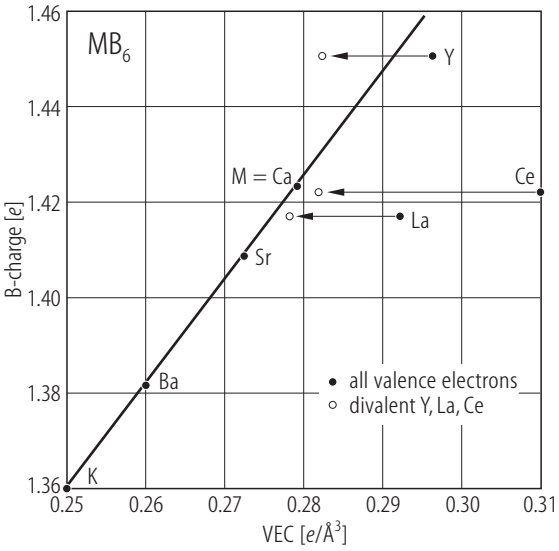

Fig. 7.

Metal hexaborides. The magnitude of the ^{11}B nuclear electric quadrupole interaction (e^2qQ) in divalent- and trivalent-metal hexaborides and mixed-valent SmB_6 vs. lattice parameter [86B]. The right ordinate $|eq|$ shows the magnitude of the electric field gradient at the boron nucleus converted from $|e^2qQ|$. Broken and dotted curves: theoretical calculations [79A].

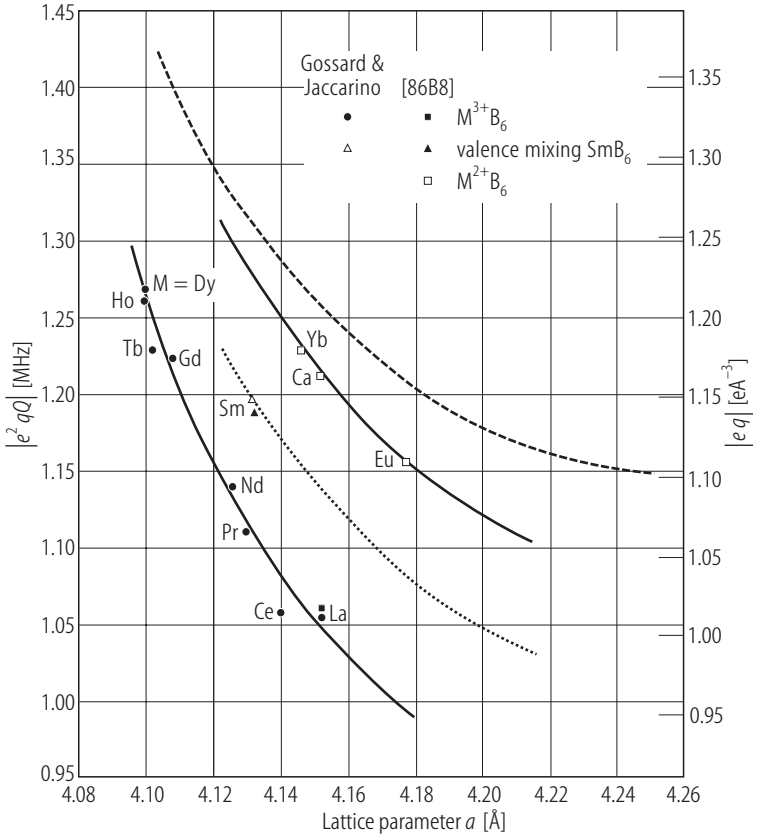

Fig. 8.

Metal hexaborides. **(a)** Work function and **(b)** effective magnetic moment vs. atomic number [59S].

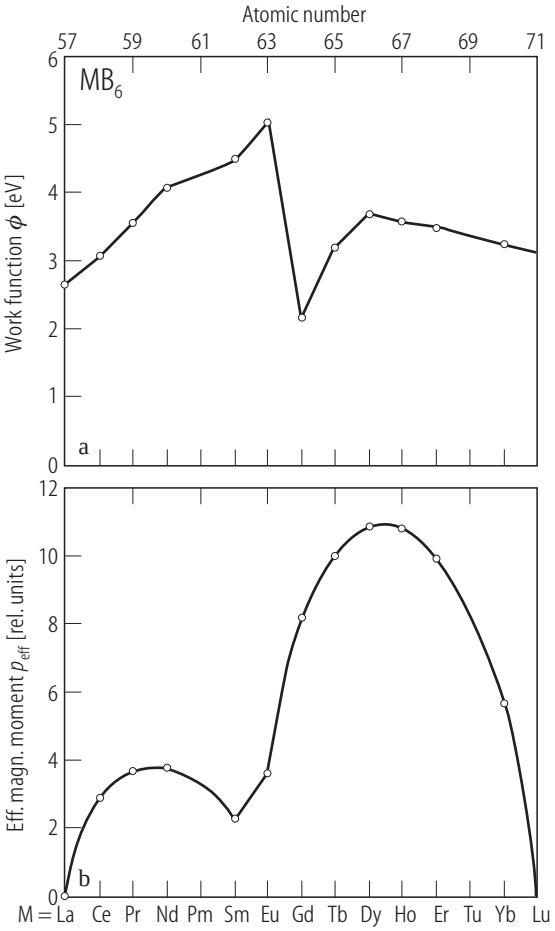

Fig. 9.

Metal hexaborides. Optical reflectivity spectra; *R* vs. photon energy. Long-dashed curve, LaB_6, solid curve, SmB_6, short-dashed curve, EuB_6 [81S].

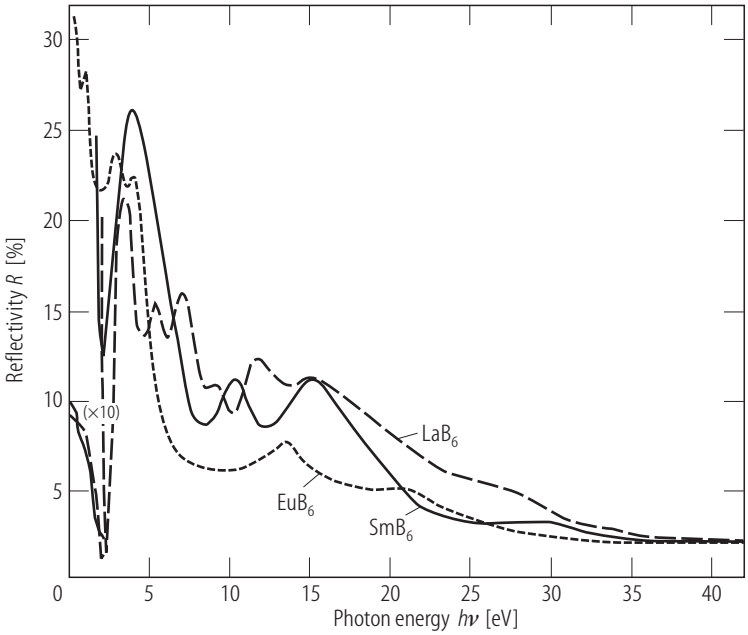

Fig. 10.

Metal-hexaborides (metallic). IR reflectivity spectra of single-crystal pure YB_6, LaB_6, CeB_6, SmB_6, $Sm_{0.8}B_6$ and TbB_6.. Some of the spectra are vertically shifted to avoid superposition. The amount of the shift is indicated at the spectra in the diagram. It is assumed that the phonon spectra occur in the spectra because symmetry selection rules are lifted in consequence of structural distortions [99W].

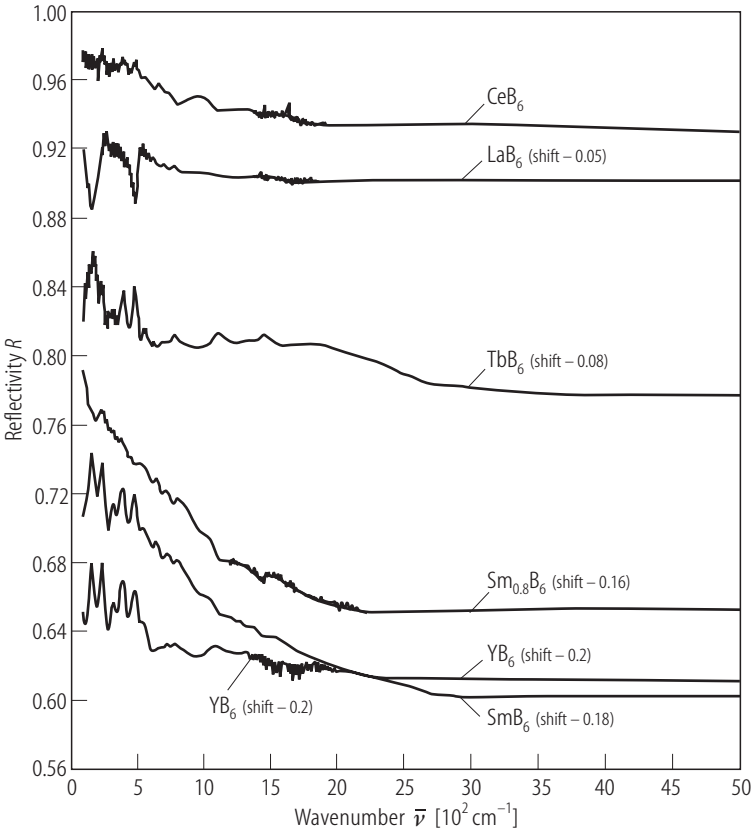

Fig. 11.

Metal hexaborides. IR diffuse reflectance spectra of representative MB_6 compounds with two-valent Ca, Sr and Yb, and three-valent Nd, Gd, La, Tb and Dy metal atoms [88T, 93Y].

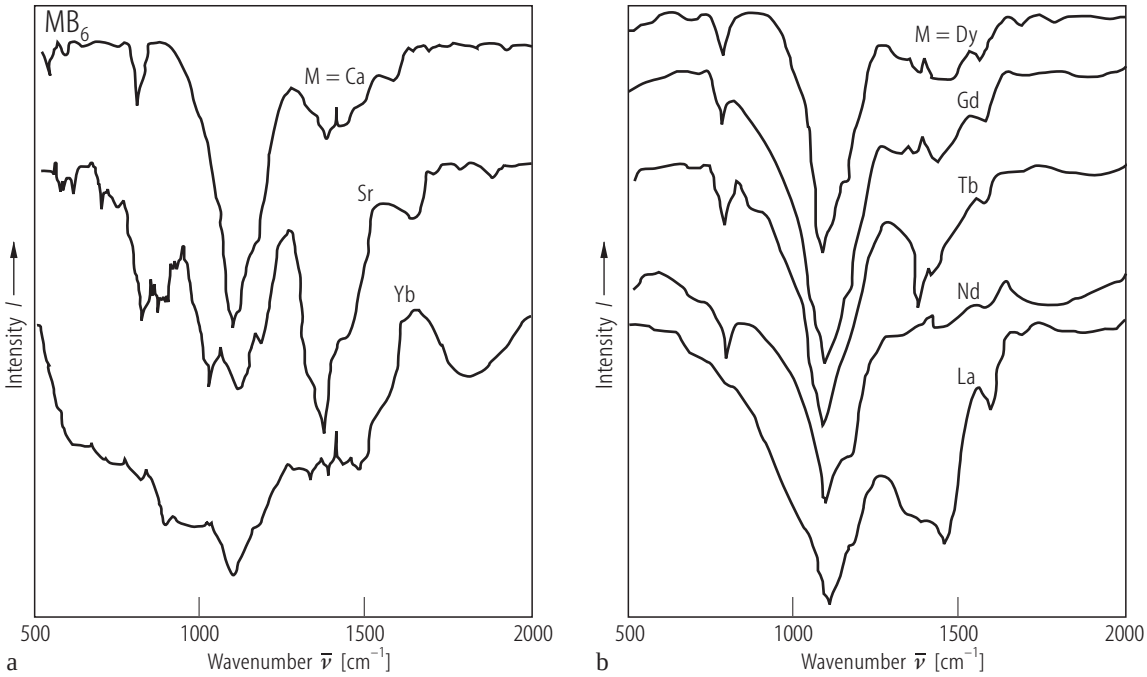

Fig. 12.

Metal hexaborides. Raman spectra, relative intensity vs. Raman shift for hexaborides with twofold and threefold ionized metal atoms [88T, 93Y].

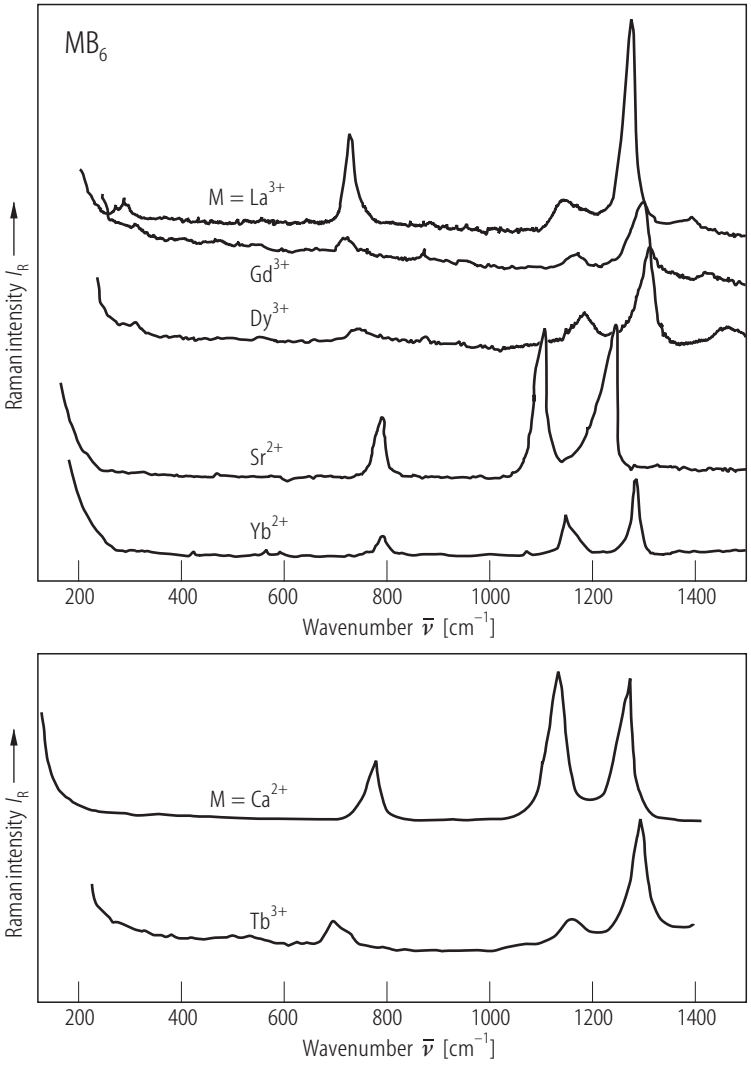

Fig. 13.

Metal hexaborides. Wavenumbers of the phonon symmetry modes A_{1g}, E_g, T_{2g} and T_{1u} vs. lattice parameter for divalent EuB_6, intermediate valent SmB_6 and trivalent YB_6, GdB_6, NdB_6, CeB_6 and LaB_6 [86Z]. Circles, experimental data; solid lines, averaged and extrapolated; dashed lines, assumed variation based on the experimental data for EuB_6.

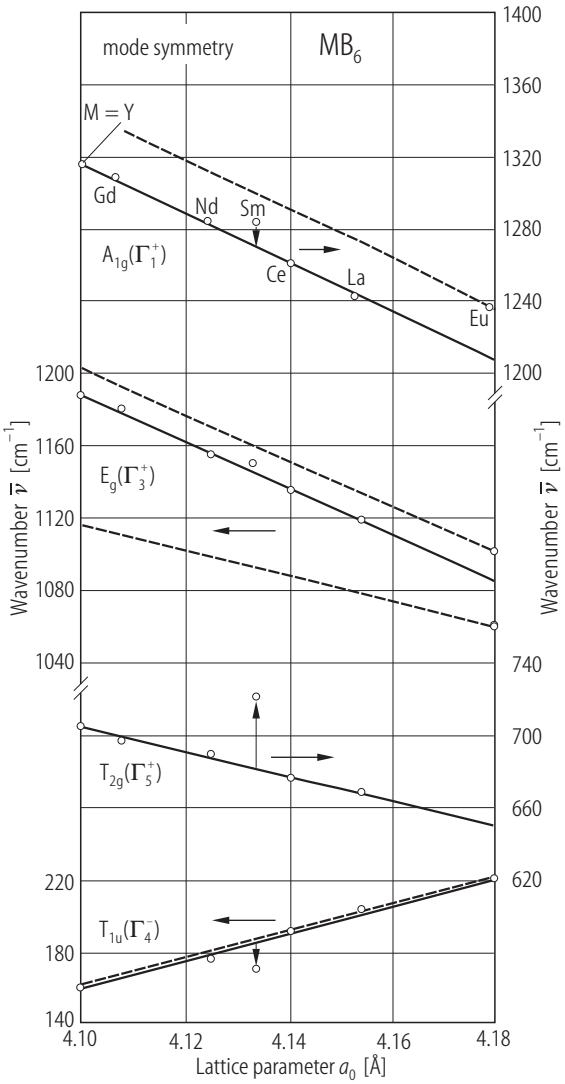

Fig. 14.

Metal hexaborides. Phonon frequencies obtained from the IR absorption spectra (calculated from the measured reflectivity spectra in Fig. 10 by Kramers-Kronig transformation). Same symbols are used for phonons in different compounds, which can be probably attributed to one another. The dashed lines represent the Raman frequencies in Fig. 11. The full lines combine the plasmon polariton frequencies of the semiconducting hexaborides EuB_6 and YbB_6, and the arrows indicate the shift to the related resonance frequency in metallic LaB_6 (softening of the high frequency F_{1u} mode and hardening of the low frequency F_{1u} mode) obviously caused by the high carrier concentration [99W].

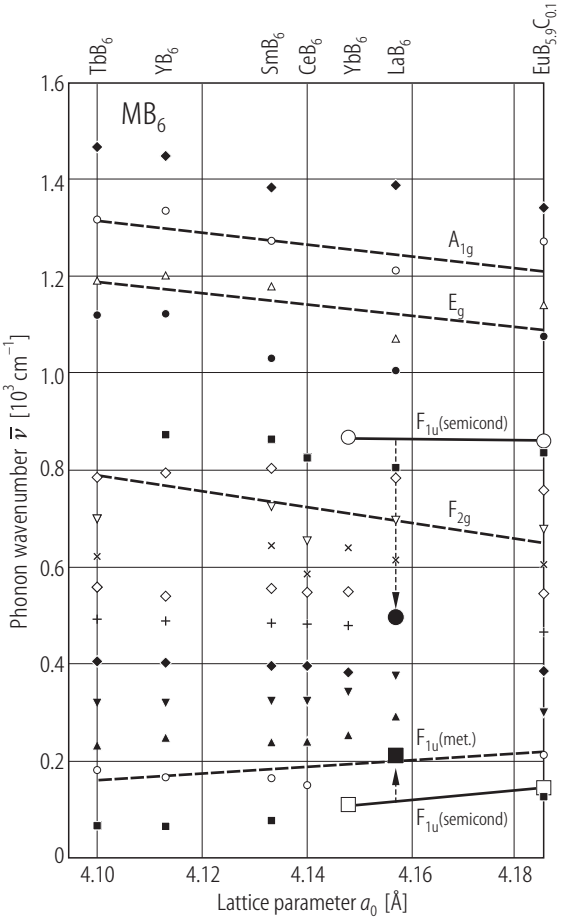

Fig. 15.

Metal hexaborides. Inverse molar magnetic susceptibility; χ_m^{-1} vs. T [97T]. χ_m in CGS-emu.

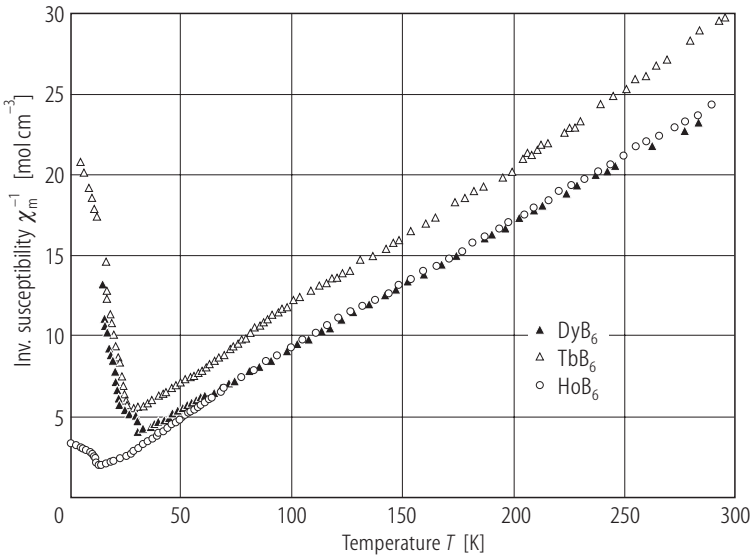

Fig. 16.

Metal hexaborides. Pressure dependence of the electrical resistivity; $\rho(p)/\rho(0)$ vs. hydrostatic pressure p. Full lines, monocrystalline LaB_6, EuB_6 and YbB_6 [91S], dashed lines, LaB_6, SmB_6 prepared from starting ratios Sm:B 1/7, 1/9, 1/12 (effect increases this way), YbB_6, EuB_6 [81K].

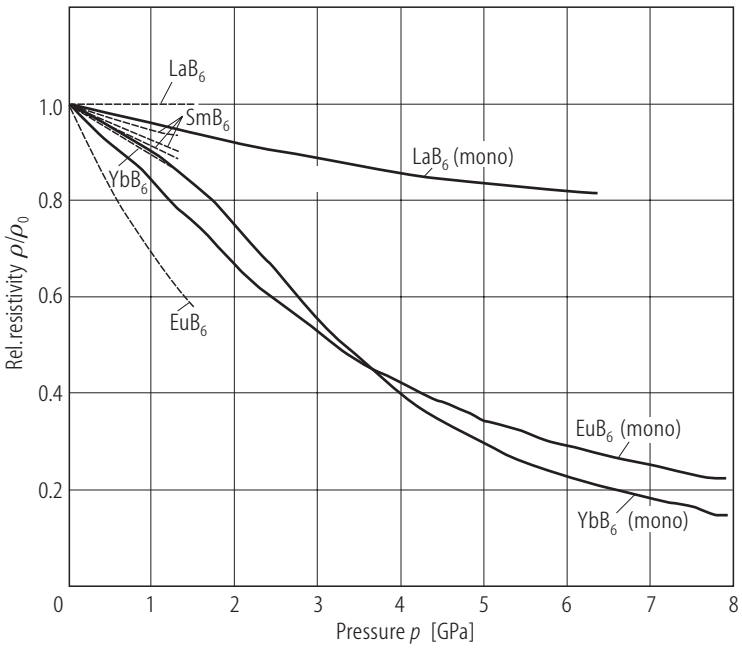

Fig. 17.

Metal hexaborides. Pressure dependence of the thermoelectric power S for LaB_6, YbB_6 and EuB_6 [81K].

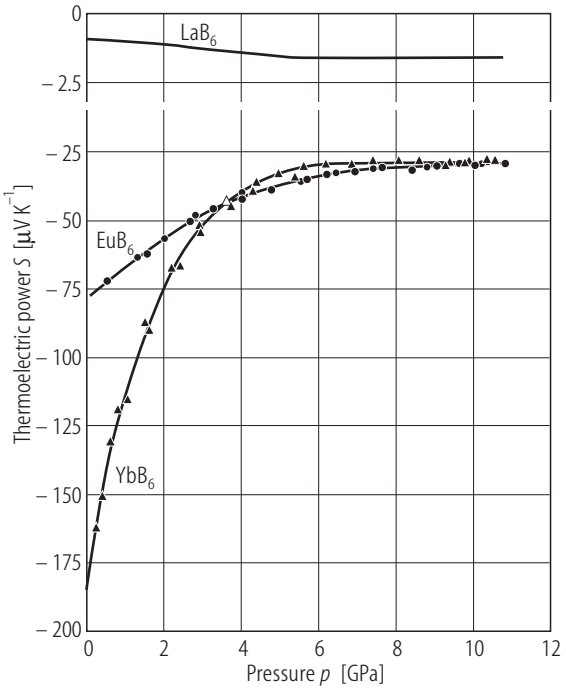

Fig. 18.

Metal hexaborides. Boron-boron bond lengths vs. lattice parameter *a* (full triangles, hypothetical equidistance) [94K].

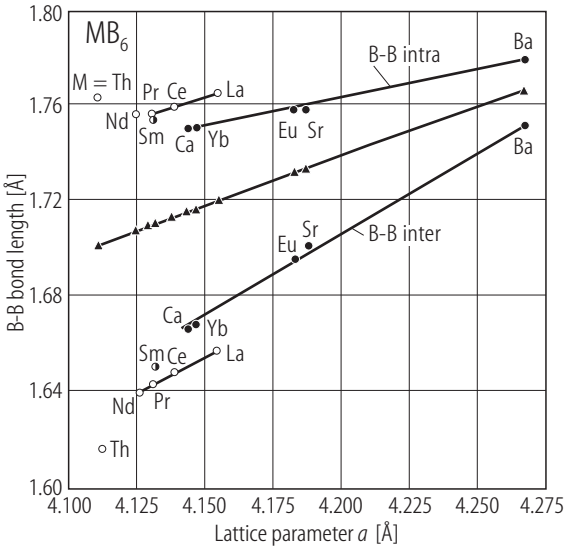

Fig. 19.

Metal hexaborides. Characteristic Einstein temperatures of the Ln atoms vs. atomic number of the Ln element; full circles [94K]; triangles [99T].

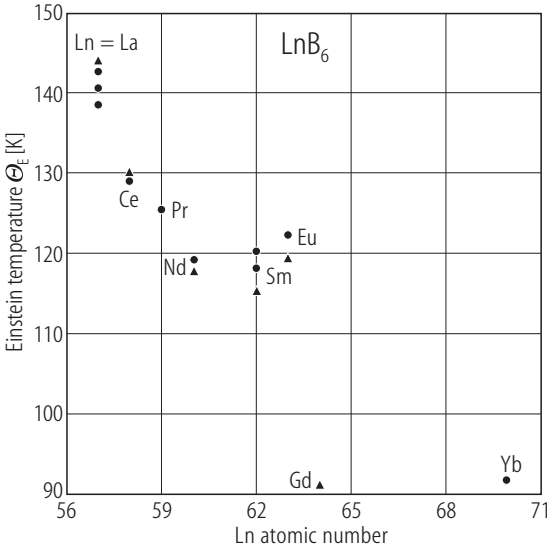

Fig. 20.

Metal hexaborides. Variation of the atomic equivalent temperature factors (normalized by a^2) vs. the atomic number of the Ln element (full circles, Ln atom; open circles, B atom) [94K].

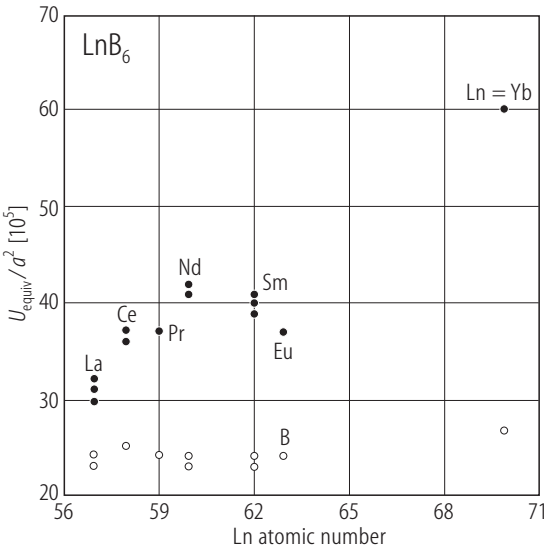

Fig. 21.

Metal hexaborides. Entropy vs. T for LaB_6, ferromagnetic EuB_6, antiferromagnetic EuB_6 [80F].